Application Notes

Structure of Intriguing Meso-Microporous Zeolites

Zeolite with small and medium-sized pores acts like a funnel, enhancing its catalytic properties

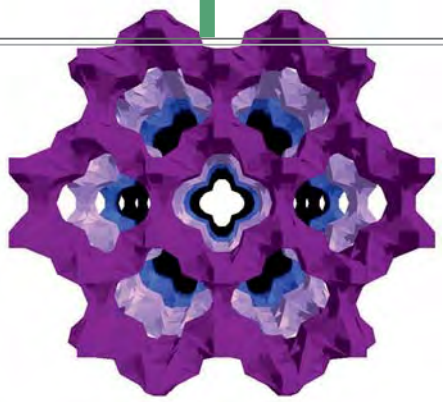

meso-microporous ITQ-43

Zeolites are crystals that are mainly created from aluminum and silicate. They have small pores which make them interesting for the field of energy and environmental technology due to their potential use as adsorbers, ion exchangers or catalysts. In water treatment, they can help to filter out heavy metals; in the oil and gas industry, their introduction was like a mini revolution for crude oil cracking. We also encounter them in our everyday lives inside washing powders .

The challenge:	nanocrystalline powder with very poor X-ray diffraction pattern; crystal degradation at ambient temperature
Solution:	3D diffraction Tomography & precession electron diffraction with a cryo- holder

As catalysts, Zeolites are not effective for processing large molecules as these cannot enter inside the pores. To overcome this obstacle several strategies have been considered, such as increasing the pore dimensions and increasing the ratio of the external to internal surface by decreasing the crystallite size or by preparing monolayered zeolites . Another approach is to generate mesopores within the zeolite crystallites, yielding a network of connected mesopores and micropores. Such networks can improve the activity and selectivity of catalysts for cracking and hydrocracking of vacuum gasoil.

Avelino Corma and his research group from the Technical University of Valencia synthesized a zeolite with small and medium-sized pores, the combination of which acts like a funnel, thereby further enhancing its catalytic properties. The zeolite ITQ-43 that features a structurally hierarchical system of connected mesopores and micropores, was synthesized as a silicogermanate.

Due to large cell parameters, data resolution of X-ray Powder Diffraction was reduced by severe peak overlap even at low 2q values (dmin > 1.8 Å). In combination with the low stability of the calcined sample, this precluded the extraction of an appropriate set of intensities for structural determination using powder data. Thus, 3D diffraction tomography strategy in combination with beam precession was applied for structure solution of the ITQ-43 zeolite.

Diffraction tomography data was collected from two different crystals by cooling the sample down to liquid N_2 temperature (~100 K). The three-dimensional reconstructed volume revealed only extinctions due to C-centering. Reflection intensity symmetry was consistent with Laue class Cmmm, confirming the orthorhombic setting (Rsym= 24%). ITQ-43 has a very open structure, with a framework density as low as 11.4 tetrahedral atoms per 1000 $Å^3$. The most notable characteristic of ITQ-43 is the leaf-like channels formed by 28-rings (units of 28 tetrahedral atoms) presence of clover along the c axis, with pore diameters in the range of the mesopore (21.9 Å × 19.6 Å). This mesoporous system is also connected by 12-ring channels of 6.8 Å × 6.1 Å along the a axis, and two additional sets of 12-ring channels along (a + b) and (a – b), related by symmetry, with apertures of 7.8 Å × 5.7 Å.

Even though the combination of HRTEM, electron diffraction, and XRPD data provides an important step toward the solution of complicated zeolitic structures, *ab initio* structure solution by direct methods based on pure electron diffraction data may be a faster and more reproducible path applicable to any class of catalytic porous materials.

Crystal Structure

Orthorombic Cmmm
a=26.09 Å
b=41.87 Å
c=12.84 Å

Strucural data

tilt range: ±50° step: 1°
No ind. reflections: 2735
No ind. atoms: 39
R = 34%

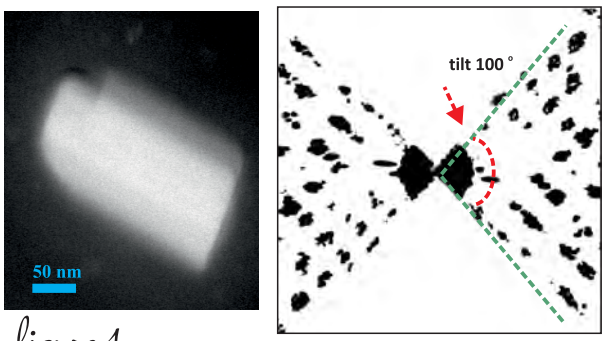

figure 1 ITQ-43 Crystal And the Corresponding 3D Reflection Reconstruction Map

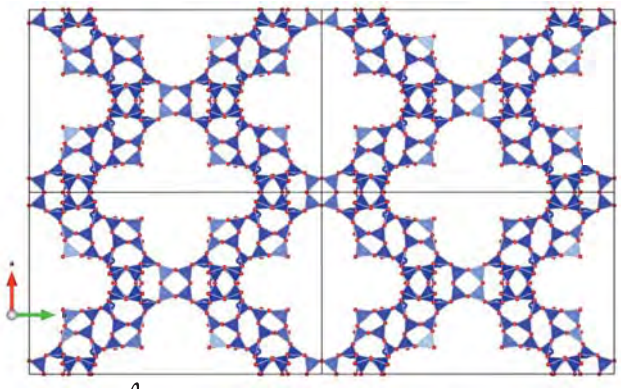

figure 2 Crystal Structure of ITQ-43

J. Jiang et al *Science* (2011) 333 1131-1134

Architecture of Hybrid Nanocrystalline Microporous Materials

Hybrid zeolites are well established as heterogeneous catalysts, ion exchangers, and molecular sieves with many different pore architectures

petrochemical Industry

The synthesis of aluminosilicate hybrids with organic groups fused within a crystalline framework is a daunting mission which has eluded many workers. Hybrids add variable chemical modification to the repertoire of zeolites, which are well established as heterogeneous catalysts, ion exchangers, and molecular sieves with many different pore architectures.

Before 2008, when the crystalline aluminosilica-based hybrid organic-inorganic porous materials -ECSs (eni carbon silicates)- were synthesized and analyzed, only hybrid materials made of amorphous siliceous were known. In 2012 a novel ECS structure was unrevealed: ECS-3. ECS-3 has textural properties typical of a crystalline microporous material (specific surface area 296 m^2g^{-1}, specific pore volume 0.13 cm^3g^{-1}, type I N2 adsorption isotherm).

The challenge:	polycrystalline, beam sensitive & highly complex X-Ray diffraction pattern
Solution:	3D diffraction tomography and precession electron diffraction, in combination with X-Ray refinement

The structure analysis of ECS-3 ($Na_{20.8}Si_{32}Al_{24}O_{96}C_{96}\cdot 32H_2O$) proved to be most challenging as the polycrystalline material is produced as small crystals (1 µm) and provides highly complex high-resolution X-ray powder diffraction (HR-XRPD) pattern, even from synchrotron beam line. Furthermore, the extremely fast deterioration of the structure under the electron beam of a transmission electron microscope does not allow the application of conventional methods.

3D diffraction tomography technique was the tool to surmount these obstacles. The benefits of diffraction tomography are that the reduced electron dose allows data collection on beam-sensitive materials and the collected data are less affected by dynamic scattering than conventional in-zone diffraction data, especially when beam precession is applied.

Analysis of diffraction tomography data collected on a small ECS-3 crystal under stable conditions provided a monoclinic unit cell. Based on intensities extracted from 3D electron-density data, a significant portion of the ECS-3 structure was readily obtained by using Cc space group in the SIR2004 software suite. The phenylene rings were completed with the specific routines of SIR2004, while the position of the extraframework species (Na/K and H_2O) were determined by analysis of the Fourier maps generated during the Rietveld refinement of the structure performed against the HR-XRPD data with GSAS software.

Crystal Structure

$Na_{20.8}Si_{32}Al_{24}O_{96}C_{96}\cdot 32H_2O$

Monoclinic Cc
a=19.7 Å
b=27.7 Å
c=9.5 Å
β=102.78°

Experimantal data

tilt range: ±60° step: 1°
No ind. reflections: 2206
No ind. atoms: 62
R = 24.7 %

The intriguing crystal structure of ECS-3, whose framework contains 62 atoms in the asymmetric unit, is one of the most complex structures ever solved by electron diffraction, with a structural complexity comparable to zeolites. This is remarkable considering the high beam sensitivity of the sample, due to the phenylene rings. 3D diffraction tomography was indeed indispensable and could become widely utilized for structural investigation of hybrid nanocrystalline microporous materials.

figure 1

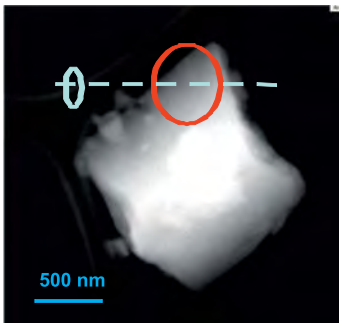

ECS-3 Crystal & Tilted Area used 3D Diffraction Tomography

figure 2

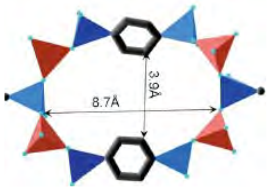

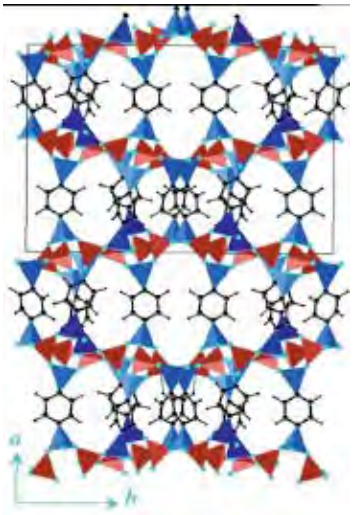

Left: ellipsoidal ring of the sinusoidal channel snaking along [001]. Right: [001] projection of the ECS-3 framework structure.

G. Bellussi et al *Angew. Chem. Int. Ed.* (2012) 51 666 –669

From "Clean Energy" Cars to Structure of Metal-Organic Framework Materials (MOFs)

Hydrogen is able to replace petroleum in the future. However, hydrogen storage is a difficult problem which still has to be solved

Fossil fuel energy sources and their burning emissions from vehicles have a very negative impact on the environment and on people's health. Furthermore, fossil fuels are not renewable, which means that if the world use them uncontrollably, fuel will be limited in the future. Hydrogen is an attractive energy carrier which could replace petroleum. However, hydrogen storage is a difficult problem which still has to be solved. Investigation of metal-organic frameworks (MOFs) as porous materials for hydrogen storage is currently an important research field. Due to a recent requirement of United States Department of Energy, a hydrogen storage tank must contain 6 wt% of hydrogen. Hydrogen uptake depends on several properties of porous material. However, a material with a high surface area or free volume alone is not necessarily a good candidate for hydrogen storage. Pore size distribution of MOF strongly influences the heat of adsorption. Thus, frameworks with smaller pore sizes have higher heat of adsorption due to a stronger interaction between adsorbed hydrogen molecules and cavities. The desorption temperature of hydrogen increases likewise with decreasing pore size. Calculations showed that pores with diameter of 7 Å should be optimal for hydrogen adsorption. Additionally, the stability of metal-organic framework plays a very important role for its potential use as hydrogen storage material as well as for other applications.

The challenge:	MOF are nanosized crystals & extremely beam sensitive
Solution:	3D Diffraction Tomography & precession electron diffraction with a cryo-holder used for keeping the temperature at ~100K

Triazolate-based MOF featuring Kuratowsky-type secondary building units, have been studied thoroughly. MFU-4, constructed from benzobistriazolate linkers and $\{Zn_5Cl_4\}^{6+}$ cores, features a very high thermal and hydrolytic stability. Due to its small pore apertures (2.5 Å) it is highly selective for the adsorption of atoms or small molecules such as H_2. However, in order to separate mixtures of larger molecular adsorbates for catalytic transformations, a porous framework featuring larger pore apertures is required. MFU-4l(arge) $[Zn_5Cl_4(BTDD)_3]$ constructed by a longer triazolate linker compared to MFU-4, is a novel member of isoreticular MFU-4-type frameworks that has been studied recently.

The crystal structure of MFU-4l has been solved *ab initio* from powder X-ray diffraction data by direct methods. An independent structure analysis was performed by 3D Electron Diffraction Tomography in parallel, using a cryo-holder to avoid sample melting due to beam exposure.

The crystal structure of MFU-4l is similar to that of MFU-4 in that it possesses a cubic six-connected net.

Thermogravimetric and VTXRPD analyses indicate that MFU-4l possesses very high thermal stability (500 °C under nitrogen). Large pore apertures of 9.1 Å allow adsorption and free diffusion of different molecules. In contrast, MFU-4, presenting small pore apertures of 2.5 Å, is highly selective for the adsorption of atoms or small molecules such as He or H_2. MFU-4l, which has a much higher surface area, is generally able to adsorb more hydrogen than MFU-4. However, at higher temperatures and lower pressures MFU-4 adsorbs more hydrogen than MFU-4l. Thus, MFU-4 is more suitable for hydrogen adsorption than MFU-4l. It has been demonstrated that MFU-4-type of frameworks have a huge potential for the development of functional materials for hydrogen storage, gas separation (MFU-4) and possible catalytic applications (MFU-4l).

Crystal Structure

$Zn_5Cl_4(BTDD)_3$

Cubic Fm-3m
a=31.057 Å

Experimental data

tilt range:±60°step: 1°
No ind. reflections: 412
No ind. atoms: 9
R = 32.1 %

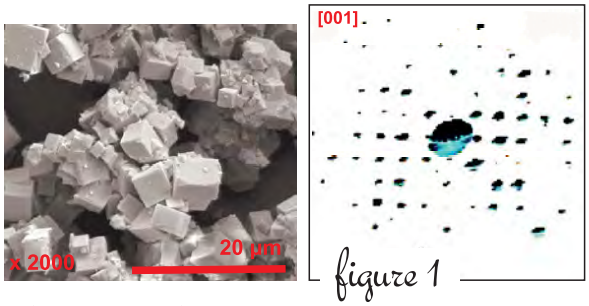

figure 1

SEM image of MFU-4l & 3D Diffraction Reconstruction

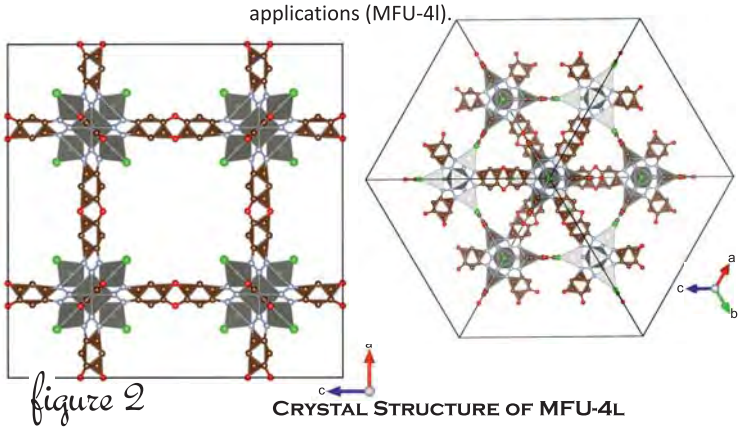

figure 2

Crystal Structure of MFU-4l

D. Denysenko et al *Chem. Eur. J.* (2011) 17 1837-1848

Inside the Structure of Dye-Sensitized Solar Cells

TiO_2 nanoparticles have been utilized in a multitude of applications, photocatalysis, dye-sensitized solar cells, gas sensors, hydrogen storage etc

Dye-sensitized solar cells (DSSCs) belong to the family of thin film solar cells and are an attractive and a considerably cheaper way of producing electricity. DSSCs are designed like a traditional alkaline battery and do not require a tricky manufacturing process. They are produced by a porous titanium dioxide nano particles layer. This layer is covered with a molecular dye that can absorb sunlight, and is submerged in an electrolyte solution with a platinum-based catalyst above it. When sunlight passes through the cell and reaches the dye layer, it activates electrons, which then enter the titanium dioxide layer.

The challenge:	nanocrystalline domains in structurally disordered wires; low X-Ray pattern quality
Solution:	Automated 3D Diffraction tomography & Precession Electron Diffraction

Then these electrons flow towards the transparent electrode and get collected in order to power a load. The electrons flow through the external circuit and then re-enter the cell on a metal electrode to flow into the electrolyte, which then transports them back to the dye molecules.

In order to obtain highly efficient DSSCs two counteracting requirements have to be met. First a large number of dye/ semiconductor interfaces are needed to ensure a high photocurrent (i.e. high surface area), and at the same time a high transport rate of electrons towards the front electrode is essential . By using TiO_2 nanorods as an additive to the commonly used nanoparticular TiO_2 semiconductor, these demands can be met.

Sodium titanate nanorods represent an important intermediate product in the synthesis of TiO_2 nanorods. Despite the importance of sodium titanate nanorods as a precursor for long TiO_2 nanorods, little effort has been made to investigate the crystal structure of these nanostructures. X-ray powder diffraction crystalography failed to resolve the structure of such nanorods due to the often low-quality of data, which renders a real phase determination very difficult.

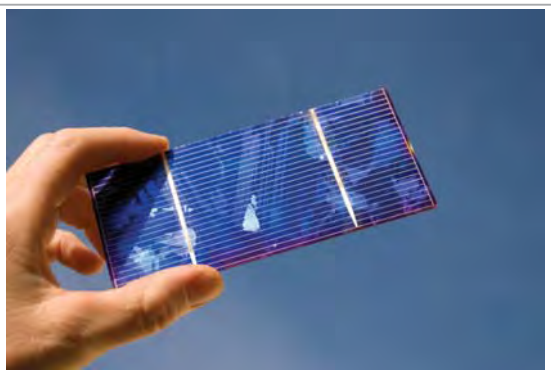

Dye-Sensitized Solar Cell

The structure of $NaTi_3O_6(OH)_2H_2O$ nanorods was determined using electron diffraction data collected by 3D diffraction tomography. Electron diffraction tomography is able to deliver in an automated way rich and quasi-kinematical electron diffraction data sets from single nanocrystals.

3D diffraction tomography data sets were collected from six different rods with different rate of disorder. The structure determination was performed on the basis of the more ordered data set. C2/m was chosen as the correct space group and the corresponding solution was used for further refinement. All maxima in the electron density distribution of the obtained structure model are located on a mirror plane (y = 0.0 or 0.5). The three strongest maxima detected in the centres of the octahedra were assigned to the Ti atoms. The remaining weaker maxima were assigned to O, Na and water molecules of crystallization. The final structure consists of groups of corrugated layers of corner- and edge-sharing $\{TiO_6\}$ octahedra arranged parallel to the (001) plane.

Crystal Structure

$NaTi_3O_6(OH)_2H_2O$

Monoclinic C2/m
a=21.53 Å
b=3.79 Å
c=11.92 Å
β=136.3°

Experimental data

tilt range: ±60° step: 1°
No ind. reflections: 628
No ind. atoms: 13
R = 35.8 %

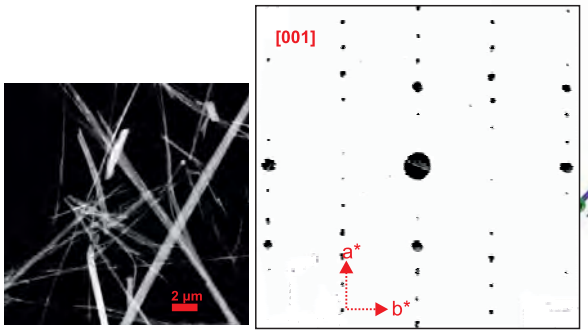

figure 1

STEM Image of Nanorods & (001)Projection of 3D reconstruction reciprocal space through ADT data set

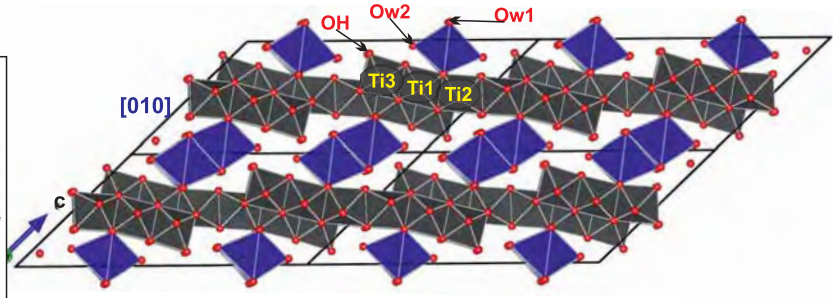

figure 2

Model of $NaTi_3O_6(OH)_2H_2O$ (view in [010]). H atoms omitted. $\{NaO_6\}$ octahedra are viewed edge-on. Hydrogen bonds are drawn as dotted line

I. Andrusenko et al *Acta Cryst.* (2011) B67 218–225

Towards Alternative Energy Sources: Structure of Thermoelectric Nanomaterials

Thermoelectric materials allow the conversion of a thermal gradient into a gradient of electrical potential

solar cells

The decrease of fossil fuel resources has motivated many research groups to seek technologies for the utilization of alternative energy sources. Solar cells operating at 20% efficiency and covering 0.1% of the Earth's land area would be sufficient to supply the worldwide yearly energy requirement . The Sun as an energy source can also be used by thermoelectric (TE) modules which directly convert solar heat into electricity. The advantage of TE modules compared to photovoltaic (PV) solar cells is that TE modules utilize the whole solar spectrum (IR, UV and visible radiation), while PV cells only use the UV–Vis part of the spectrum Low thermal conductivity is a prerequisite for effective thermoelectric materials, and the challenge is to limit the transport of heat by phonons, without simultaneously decreasing charge transport. Zinc antimonides, like Zn_4Sb_3 and ZnSb are well known thermoelectric materials as they have a high potential as the p-type leg of thermoelectric couples and are used to generate electric power in a temperature range of 300K to 700K. The thermoelectric power factor of ZnSb is high enough to make it a attractive thermoelectric material. A solution-phase technique was devised for synthesis of Zn_4Sb_3 nanocrystals as a precursor for phase segregation into ZnSb and a new Zn-Sb intermetallic phase, $Zn_{1+\delta}Sb$, in a peritectoid reaction. Crystallographic investigation of the synthetic modules was performed using electron diffraction, as single-crystal X-ray diffraction techniques cannot be applied to nanostructures and powder X-ray analysis meets serious problems when the size of the crystals is below 50 nm and there is the probable presence of different phases in the sample.

The challenge:	aggregated of polyphasic nanoparticles; low quality X-Ray pattern
Solution:	3D diffraction Tomography with precession diffraction

The TEM data show clearly the presence of at least two crystalline phases. The unit cell parameters of the first phase, ZnSb, were determined with the 3D diffraction tomography data and subsequently refined against powder X-ray diffraction data. They agree well with the known structure. The systematic extinctions on the 3D reciprocal spare are compatible with the space group Pbca and the obtained structure model exhibits a close match to the known crystal structure of ZnSb with errors in atomic positions of 0.02 Å for Sb and 0.05 Å for Zn.

The 3D reconstructed data set recorded for the unknown second phase, $Zn_{1+\delta}Sb$, shows that the cell parameters did not match those of any known Zn-Sb phase, even if the new phase has to be strictly geometrically related with rombohedral Zn_6Sb_5. A careful inspection of several zone axes using beam precession shows that the only true symmetry element present is the inversion center, and the structure is triclinic. Processing 3D diffraction tomography & PED data using Sir2008 the structure was finally solved in space group P-1. A fully kinematical approach was used, and no correction was applied to the data set.

Ab initio structure solutions were performed for both the phases on the basis of electron diffraction data obtained by ADT. Precession electron diffraction data were necessary for the more complex phase $Zn_{1+\delta}Sb$. This new $Zn_{1+\delta}Sb$ phase crystallizes with a hexagonal pseudosymmetry in the triclinic space group P-1 and shows strict relations with both $Zn_{13}Sb_{10}$ and ZnSb. Remarkably, the structure was obtained by single- crystal analysis of a 50 nm particle, and the solution was achieved *ab initio* in one step with a fully kinematical approach.

Crystal Structure

$Zn_{1+\delta}Sb$

Triclinic P-1
a=15.31 Å
b=15.51 Å
c=7.81 Å
α= 88.87°
β=89,42°
γ=119.4°

Experimental data

tilt range: ±38° step: 1°
No ind. reflections: 3651
No ind. atoms: 30
R = 36.19 %

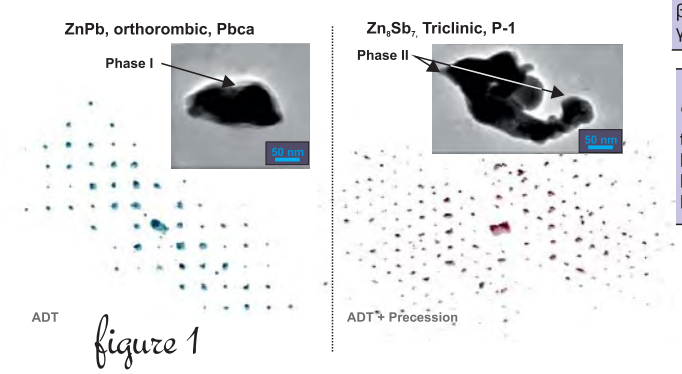

figure 1

Nanocrystals Area used for Structure Analysis and the Corresponding 3dDiffraction reconstruction of Phase I (Left) & Phase II (Right)

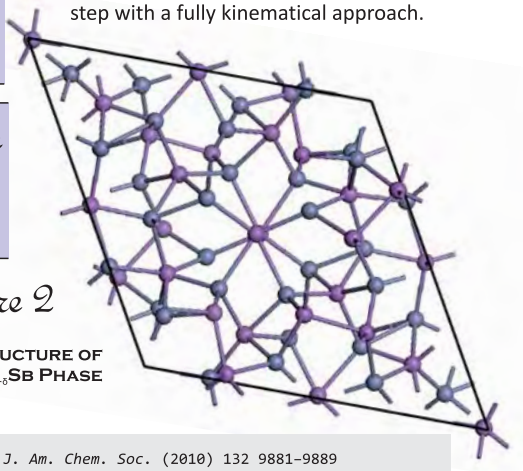

figure 2

Crystal Structure of the $Zn_{1+\delta}Sb$ Phase

C. S. Birkel et al *J. Am. Chem. Soc.* (2010) 132 9881–9889

Inside the Structure of phosphor-converted light-emitting diodes (LED)

pcLEDs alow low production cost, and high colour rendering

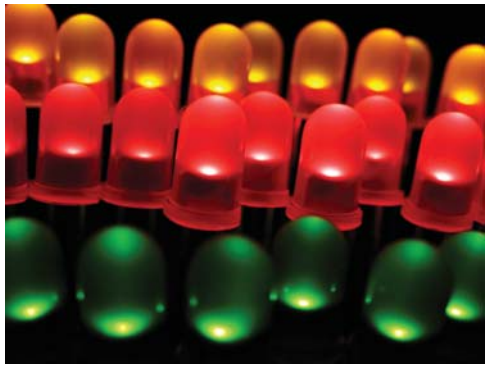

LED lights

Phosphor-converted Light-Emitting Diodes (pcLEDs) use one short wavelength LED (usually blue or ultraviolet) in combination with a phosphor, which absorbs a portion of the blue light and emits a broader spectrum of white light. The major advantage is the low production cost, and high colour rendering, while the disadvantage is the inability to vigorously change the character of the light and the fact that phosphor conversion diminishes the efficiency of the device.

The challenge:	small nano crystallites; presence of several phases
Solution:	Automated 3D diffraction Tomography & Precession Electron Diffraction

The low cost and adequate performance makes it the most widely used technology for general lighting today.

Silicates are omnipresent in everyday life due to their abundance and diversity, and play an important role in future technologies as for example the phosphors silicates to the phosphor-converted light-emitting diodes (pcLEDs) field. As SiO_2 and Phosphorus Oxide Nitride (PON) are isoelectronic, the silicate analogous compound class of oxonitrido-phosphates can be expected to exhibit a similar structural richness to the silicates. Moreover, only relatively few oxonitridophosphates have been characterized to date, as there are fundamental difficulties in terms of their synthesis. Furthermore, typical reaction products show poor crystallinity and samples notoriously contain nanosized crystals of the desired compounds accompanied by further unknown side phases. Structure elucidation of the novel oxonitrido-phosphates SrP_3N_5O and was performed *ab initio* by 3D electron diffraction tomography data collection.

$SrP_3N_5O$was obtained as nanocrystalline powder with needle-shaped crystallites in polyphasic mixtures. Two tilt series with approximately orthogonal tilt axes were recorded from the tip of a nanosized crystal needle. Each measurement was carried out using precession electron diffraction (PED) for a further reduction of dynamical scattering effects and a more appropriate reflection integration.

The obtained structure for SrP_3N_5O clearly showed an inversion center, therefore the centrosymmetric space group Pnma was selected for the final model. Twenty-five independent atomic positions were obtained and correctly identified (four Sr, six P, and fifteen O/N). Thus the complete structure including all light atoms was obtained. The structure consists of triangular columns that run along [010] that are interconnected to form corrugated layers that extend parallel to (100), with the Sr^{2+} ions being located between them. The compound is a highly condensed layer phosphate with a degree of condensation k=½. The Sr^{2+} ions are located between the layers and exhibit six-, eight-, and ninefold coordination.

Many further oxonitrido-phosphate phases in their typical nanocrystalline form can now be identified by the applied procedure. With the 3D diffraction tomography & PED method, the potential of a versatile structural P/O/N chemistry could be fully exploited.

Crystal Structure

SrP_3N_5O

Orthorombic Pnma
a= 18.33 Å
b= 8.09 Å
c= 13.85 Å

Experimental data

tilt range: ±50° step: 1°
No ind. reflections: 1790
No ind. atoms: 25
Rsym: 29.9 %

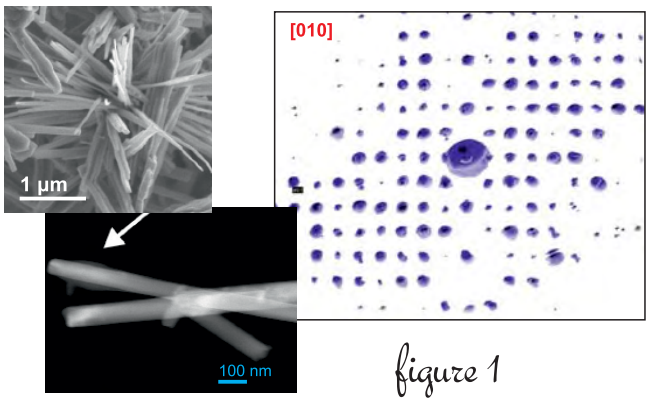

figure 1

Needle-Shaped Nanocrystals of SrP_3N_5O; Crystal for Data Collection & Corresponding 3D reconstructed Reciprocal Space

figure 2

Crystal structure of SrP_3N_5O

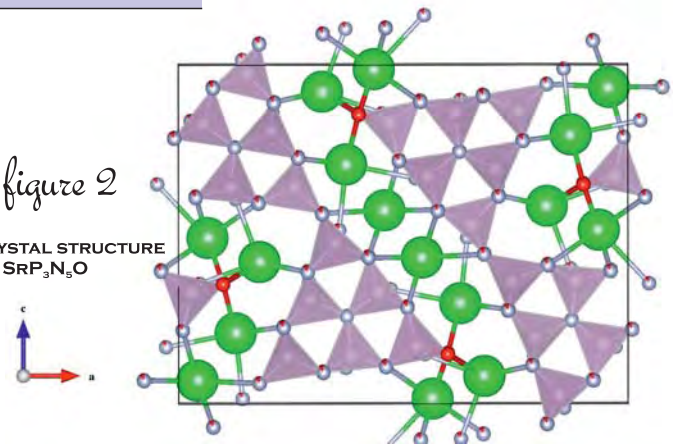

S. J. Sedlmaier et al *Chem. Eur. J.* (2011) 17 11258 – 11265

Structure of Pigment Yellow for Car Industry

Pigment Yellow 213 existing in two polymorphs is a new water-based coating compound

pigment yellow

Some years ago, automotive industry turned their interest from solvent-based to water-based coatings. This led to the requirement of novel water-dispersible pigments. Greenish-yellow shades appeared to be one of the most problematic, because all existing greenish-yellow pigments were either not dispersible in water or had an insufficient weather fastness, i.e. they faded out after a few years. Moreover, clear greenish-yellow shades cannot be achieved by mixing green and yellow pigments, since this would lead to dull shades. Due to these demands at the beginning of the last decade the Pigment Yellow 213 was developed (P.Y. 213, $C_{23}H_{21}N_5O_9$) as a new compound for water-based coatings. P.Y. 213 exists in at least in two polymorphs: the brown β-phase is formed as an intermediate product during synthesis. Subsequent heating in organic solvents to 423– 473 °K results in the greenish-yellow (lemon-yellow) α-phase. The phase shows good weather fastness and it does not agglomerate in water. Currently the α-phase is industrially used for water-based car coatings.

The challenge:	no single crystal due to low solubility; beam sensitivity; very low X-Ray pattern quality
Solution:	Automated 3D Diffraction Tomography in combination to X-Ray diffraction

Crystal structures of P.Y. 213 are not known. All attempts to grow single crystals failed, due to non-solubility in water or organic solvents, even at high temperatures. Furthermore, crystal growth from the melt or by sublimation is not possible either, because the pigment melts at 642 K with decomposition and does not sublime. The crystallinity of P.Y. 213 is never good, and thus X-ray powder data alone cannot be used directly for structure analysis.

Electron diffraction data were collected by automated 3D diffraction tomography .

The lattice parameters were accessed through a tilt (tilting interval of ±30, step size of 1°) of the crystal around an arbitrary axis, whereby diffraction patterns were collected automatically using an automated diffraction tomography (ADT) module. The crystal structure of the α-phase was finally solved combining XRPD and ADT data by real-space methods using recent developments of the program TOPAS. The α-polymorph of P.Y. 213 crystallizes in P-1, Z = 2. The molecule is almost planar. There are two intermolecular hydrogen bonds, both involving the NH groups of the two cis-amide fragments of the quinoxalinedione fragment. One of the NH groups forms an intermolecular hydrogen bond with a C=O group of a neighboring molecule, resulting in an eight-membered ring across an inversion centre, as is frequently found for cis-amide systems, e.g. in benzimidazolones.

The structure of α-P.Y. 213 (yellow phase) has been solved by the combination of electron diffraction, crystal-structure prediction using lattice-energy minimization and X-ray powder data, proving the power of today's real space methods. The PDF analysis of the phase is in agreement with the crystal structure.

Crystal Structure

$C_{23}H_{21}N_5O_9$

Triclinic $P\bar{1}$
a= 6.90 Å
b= 11.83 Å
c= 14.06 Å
α= 81.81°
β= 81.03°
γ= 87.54°

Experimental data

tilt range: ±30° step: 1°

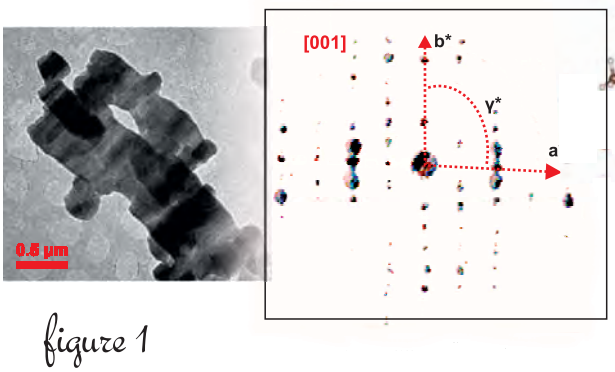

figure 1

TEM photograph of α-P.Y. 213 and 3D Reciprocal Space Reconstructed by 3D Diffraction Tomography Data

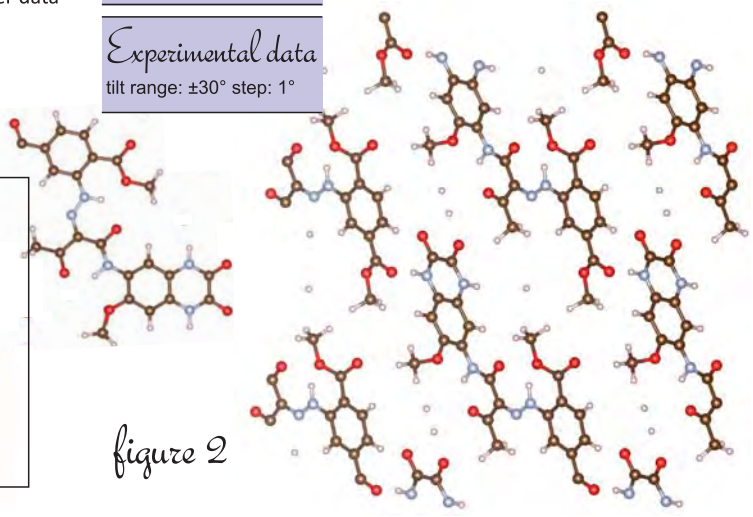

figure 2

Different Projections of Pigment Yellow 213 Crystal Structure

M. U. Schmidt et al *Acta Cryst. B* (2009) 65 189–199

Structure of Organic (CNBA) molecules

The CNBA pre-twisted conformation is responsible for its excited state dynamics

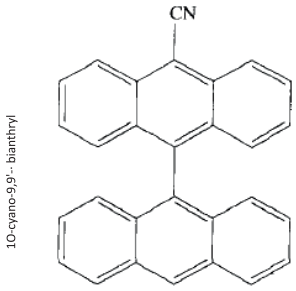

The photo-optical properties of 9,9'-bianthracene-10-carbonitrile (CNBA) in solution are related to the angle between the two anthracene moieties. The 9,9'-bianthryl and its analogues are well-known systems whose excited state behavior and dynamical processes have been studied extensively in a range of conventional solvents. The interest in 9,9'-bianthryl and its analogues is mainly due to the fact that this pre-twisted molecule with mutually perpendicular anthracene rings in the ground state undergoes symmetry breaking upon excitation and its fluorescence spectra shows distinct charge transfer character, especially in polar solvents. In nonpolar solvents the first excited state is predominantly a locally excited state with very little or no character, whereas, in highly polar solvents a charge transfer state, which is formed rapidly from the locally excited state, is the emitting state.

The challenge:	small nanocrystals; light atoms in the structure; beam sensitivity
Solution:	Automated 3D diffraction Tomography with beam precession using a cryo-holder

Information about the conformation of CNBA in the solid state can normally be obtained by X-ray crystallography. However, for many of these materials transmission electron microscopy (TEM) and electron diffraction are the only techniques because they can deliver structural information from areas as small as tens of nanometers.

While high resolution transmission electron microscopy (HRTEM) normally cannot be used with organic materials due to their fast deterioration under strong beam conditions, electron diffraction requires only a fraction of such electron dose rate on the sample. Thus, Automated 3D Electron Diffraction tomography data collection was used for structure determination of CNBA. Electron crystallography of organic materials is especially powerful, for instance, when working with polymorphic systems.

The 3D diffraction tomography data were collected in a tilt range of 120 degrees (±60 degrees), delivering a coverage of two thirds of the complete reciprocal volume. A resolution of 0.8 Å was recorded with 9415 reflections being measured which reduced to 3519 independent reflections after merging symmetry equivalents, with an Rmerge of 21.77%. Tomography data confirmed the cell parameters and allowed recognition of the space group P21 /c and solution of the structure. All the atoms (carbon and nitrogen) were detected a*b initio* with a final R of 24%.

The molecule has a rather rigid conformation. The only degree of conformational freedom is the torsion angle between the two anthracene moieties. The anthracene fragments were found basically in a flat geometry, but additional refinement of the geometry was necessary. Structure refinement was performed in SHELXS. The refinement delivered a torsion angle between the anthracene moieties of 93.8 degrees. Electron diffraction is a well-known and extremely powerful method to gain structural information from beam-sensitive materials. Although the instability of the material under irradiation means that extra care has to be taken, electron diffraction data can be collected by optimizing the acquisition conditions and result in *ab initio* structure determination

Crystal Structure

$C_{29}H_{17}N$

Monoclinic $P2_1/c$
a= 14.7 Å
b= 9.5 Å
c= 15.4 Å
β= 112.0°

Experimental data

tilt range: ±60° step: 1°
No indiv. reflections: 3519
No indiv. atoms: 30
R = 24%

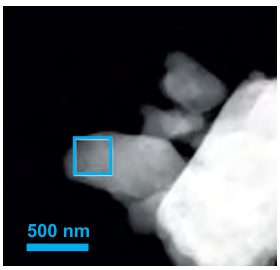

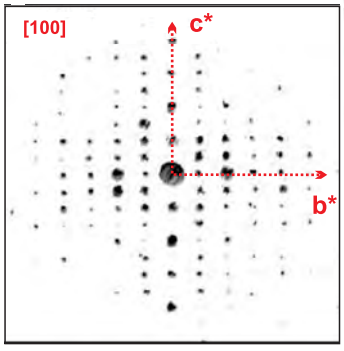

figure 1

Crystal Area Where Data collected & 3D Reconstructed Data of CNBA

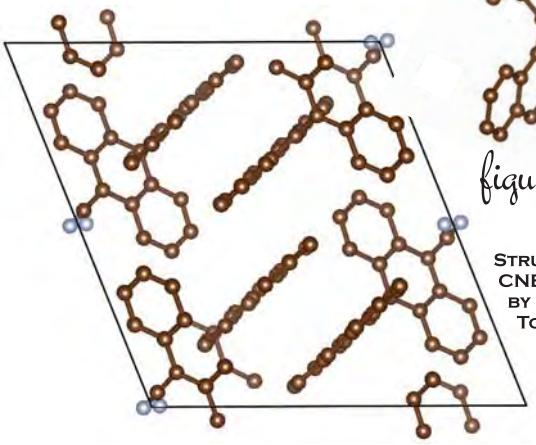

figure 2

Structure of CNBA solved by Diffraction Tomography

U. Kolb et al *Polymer Reviews* (2010) 50 385–409

Shed Light To Magma Genesis & Seismicity

Water-transfer from the subducted slab to the overlying mantle wedge leads to magma genesis & seicmicity


magma

The processes that give rise to arc magmas at convergent plate margins have long been a subject of scientific research and debate. H_2O-transfer from the subducted slab to the overlying mantle wedge has been largely recognized as one of the major processes driving rheological modifications of the upper mantle, affecting its petrological variability and promoting magma genesis. There is increasing evidence from the geological record that H_2O flux

The challenge:	HAPY phase can be identified in a high pressure multiphase synthetized sample
Solution:	3D diffraction tomography & precession electron diffraction

pathways through the slab-mantle interface is not a simple gravity driven transfer of H_2O from mafic rocks of the oceanic crust to ultramafic mantle wedge compositions.

The best way to investigate what is under our feet is to simulate the earth interior conditions in our laboratory. This can be done in a special press where chemical mixtures, having rock compositions, can be brought to high pressure (10-100 GPa) and high temperature (from room temperature to 2500 K) conditions. In a pilot study planned to explore the stability of chlorite, a phase of unknown chemical composition was encountered and powder diffraction pattern in a run charge synthetized at 720 °C 5.4 Gpa on a bulk composition representing a clinochlore: an anhydrous Al-bearing pyroxene. The stability of such previously unknown hydrous silicate beyond the chlorite pressure breakdown significantly promotes the H_2O transport in the subduction channel to depths exceeding 150Km.

The structure was solved using the 3D electron diffraction tomography method. A crystal of 3.5 µm of the unknown phase was selected on the basis of its chemical composition determined by EDS and characteristic interplanar distances observed in conventional electron diffraction. The structural model delivered after processing of 3D tomography / PED data by direct methods routine (Sir2008) in space group C2/c had a final residual (R) of 31%. The combination of EPMA mineral chemistry data, structural model resolved by 3D electron diffraction tomography method and refinement from XPRD data point to the mineral formula $Mg_{2.1}Al_{0.9}(OH)_2Al_{0.9}Si_{1.1}O_6$. Phase HAPY can account for H_2O-transport in high-pressure slab to- mantle interfaces, but the range of bulk compositions where this is possible largely depends on the degree of H_2O saturation, and on the effect of Fe and Ca in altering phase relationships.

The structure solution obtained with electron diffraction indicates that HAPY contains water as OH groups, therefore it can bring water to lower depth than chlorite. This information is of crucial importance for geologists, since the depth at which water is released is the key factor for magma formation in the mantle and earthquake activation. 3D diffraction tomography and precession can give a fundamental contribution to understanding how and where the magma of volcanos forms!

Crystal Structure

$Mg_{2.1}Al_{0.9}(OH)_2Al_{0.9}Si_{1.1}O_6$

Monoclinic C2/c
a=9.88 Å
b=11.63 Å
c=5.08 Å
β=111.07°

Experimental data

tilt range: ±60° step: 1°
No ind. reflections: 498
No ind. atoms: 8
R = 31%

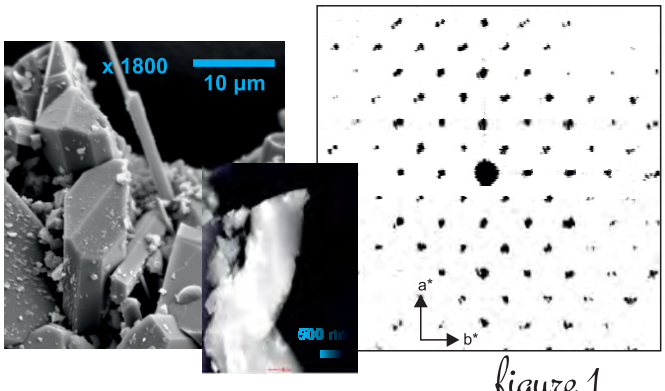

figure 1

Euhebdral Prismatic Crystals (SEM Image)
Crystal for Data Collection (STEM Image)
Corresponding 3D Reflections Reconstruction

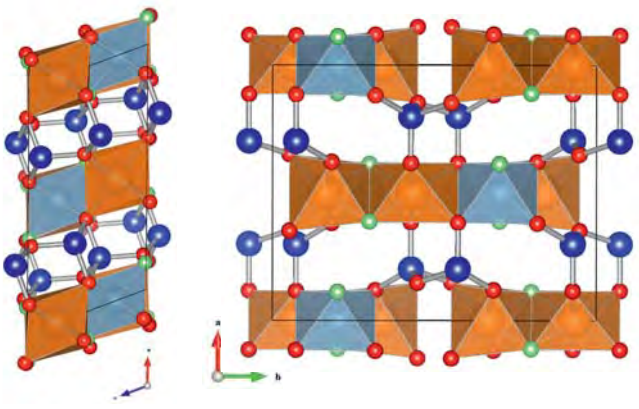

figure 2

Model of the New HAPY Phase

M. Gemmi et al *Earth and Planetary Science Lett.* (2011) 310 422–428

Charoite: The Enigmatic Structure of "Unnaturally Beautiful" Gemstone

Charoite's color ranges from lilac to violet to purple, but its unusual patterns are its distinctive signature.

Charoite is a rare mineral first described in 1978 and named after the Chara River (Murun Masif, Yakutia, Siberia, Russia). Charoite is translucent lavender to purple in color with a pearly lustre. Charoite is strictly massive in nature, and fractures are conchoidal. It has an unusual swirling, fibrous appearance, sometimes chatoyant, and that, along with its intense color, can lead many to believe at first that it is synthetic or enhanced artificially. Charoite is used as an ornamental stone and sometimes a gemstone, generally as cabochons set into pendants. However, Charoite is a discrete mineral rather than a rock.

Charoite Gemstone

The challenge:	small fiber type nanocrystals ; 2 polytypes intergrowth inside nanometric fibres; pseudosymmetries
Solution:	3D automated diffraction Tomography with precession electron diffraction with a rotational tomographic holder

Despite many attempts to solve the charoite structure, or at least to construct a convincing structural model, the structure and stoichiometry have remained enigmatic due to the presence of secondary phases, polymorphism and pseudosymmetries.

Selected area electron diffraction (SAED) patterns of different fibres along [010] have revealed the presence of four structural arrangements, presenting polytypism. The two simplest polytypic structures have clearly related cell parameters and monoclinic symmetry. These are described as 'charoite-96' and 'charoite- 90', on the basis of their β angles, respectively 96° and 90°. A third polytypic structure ('charoite-2a') was detected that present a doubling of the a- parameter in all h0l diffraction lines in SAED patterns. The presence of diffuse streaks along h0l (l = 2n+1) lines and of disordered intergrown fine lamellae in HRTEM images suggests a fourth disordered sequence of OD layers ('charoite-d').

3D electron diffraction tomography "coupled" to beam precession (PED) allowed an almost complete quasi-kinematic electron diffraction intensity collection from a single nanocrystal, allowed the structure determination of charoite for the first time.

The intensities extracted from the precessed diffraction tomography tilt series show unambiguously that charoite-90 and charoite-96 are both monoclinic, despite the β angle of 90° for charoite-90.

The angle β of 96° in the charoite-96 unit cell is produced by a shift by c/2 in comparison to the unit cell of charoite-90. Due to the spatial relationship between the octahedral bands and dreier chains this means that in charoite-96 the tetrahedral chains are shifted by c/2 along the octahedral bands in each subsequent unit cell.

Both polytypes are composed of three different silicate chains parallel to the z axis: a dreier double chain, $[Si_6O_{17}]^{-10}$, a tubular loop-branched dreie triple chain, $[Si_{12}O_{30}]^{-12}$ and a tubular hybrid dreier quadruple chain, $[Si_{17}O_{43}]^{-18}$. The chains share their apical oxygens with bands of (Ca, Na) octahedra. The K^+ and Sr^{2+} cations and H_2O molecules are located inside the channels formed by the silicate chains.

After more than 50 years of attempts to determine the enigmatic nature of the charoite structure the problem has been solved using the 3D electron diffraction tomography together with PED strategy.

Crystal Structure

Monoclinic P2,m

	cha-90	cha-96
a=	31.96 Å	32.11 Å
b=	19.64 Å	19.77 Å
c=	7.09 Å	7.23 Å
β=	90°	95.85°

Experimantal data

cha90 / cha96

tilt range: ±60° / ±60° step: 1°
No ind. reflections 2878 / 3353
No ind. atoms 90 / 89
R = 17% / 22%

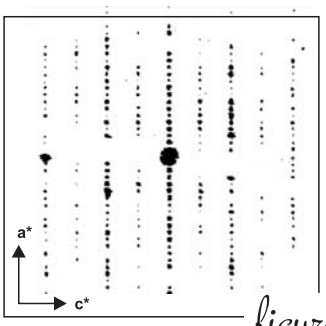

figure 1

Crystal Used for ADT Measurements.
[010] 3D reconstructed Reciprocal Space

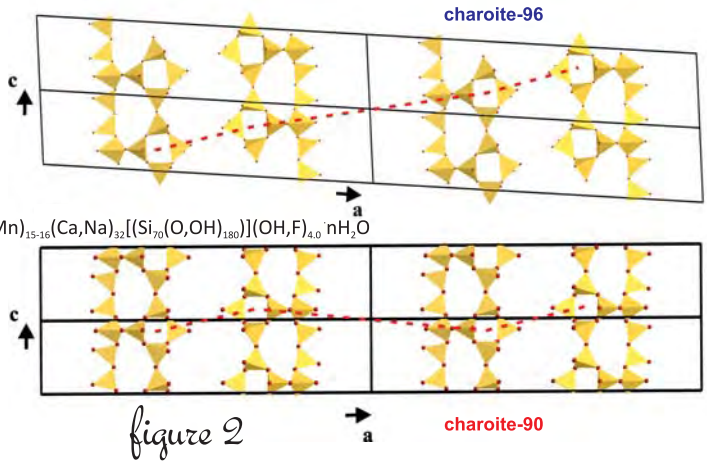

figure 2

Charoite-96 and charoite-90 polytype viewed along [010].
Only one of the drier chains is visualized.
The red line emphasizes the shift of the chain along c.

I. Rozhdestvenskaya et al *Mineral. Mag.* (2010) 74 159–177
Mineral. Mag. (2011) 75 2833–2846

Structure of New Sarrabusite Mineral

An old mine in southeastern Sardinia, is well known for the presence of an unusual number of rare secondary minerals

An old lead and arsenic mine is known at Baccu Locci near Villaputzu, in southeastern Sardinia, Italy. This locality is well known among mineralogists and collectors for the presence of an unusual number of rare secondary minerals, among which are selenites such as chalcomenite schmiederite, olsacherite and mandarinoite.

The new mineral Sarrabusite $Pb_5CuCl_4(SeO_3)_4$ has been discovered in Baccu Locci. It occurs as small lemon–yellow spherical aggregates

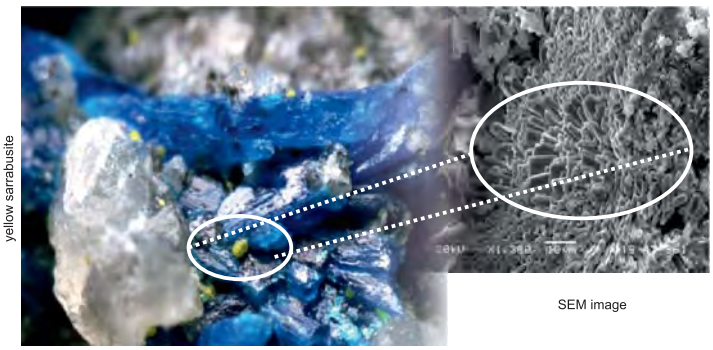

The challenge:	small crystals (< 10 µm) in small spherical aggregates; scarce sample
Solution:	Manual / Automated 3D diffraction Tomography in combination with precession electron diffraction

of tabular crystals (< 10 µm) of less than 100 µm in diameter. This mineral was discovered in the late 90's and was tentatively assigned as $Pb_4CuCl_3(SeO_3)_3(OH)$ based on EDX. However, owing to the exceedingly small dimensions, no structural study could be performed using conventional X-ray diffraction and the nature of this possibly new species remained unknown for more than a decade. The mineral and the name 'Sarrabusite' (from Sarrabus, the Sardinian region of occurrence) have been approved by the IMA Commission on New Minerals, Nomenclature and Classification of the IMA (1997-046a)

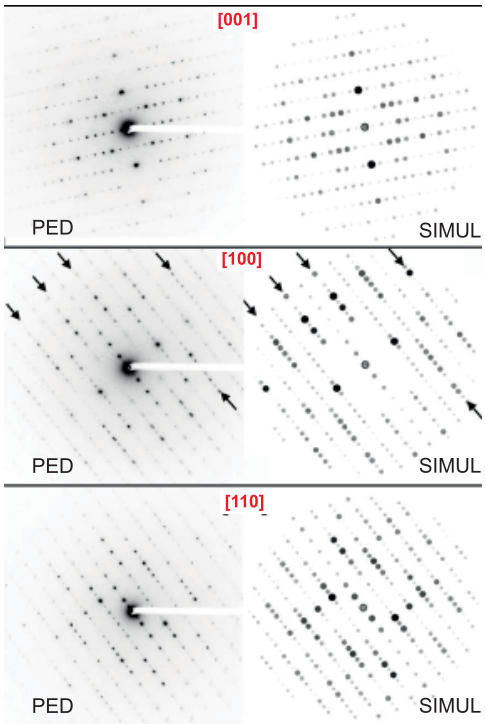

figure 1

PRECESSION ELECTRON DIFRACTION PATTERNS (LEFT) & KINEMATIC SIMULATIONS (RIGHT)

Crystal Structure

$Pb_4CuCl_3(SeO_3)_3(OH)$

Monoclinic C2/c
a=24.91 Å
b=5.50 Å
c=14.24 Å
β=101.7°

Experimental data

tilt range: ±60° step: 1°
No ind. reflections: 1515
No ind. atoms: 14
R = 32.9%

The crystal structure has been solved from and refined against electron diffraction of a microcrystal. Four data sets have been measured by both a manual and an automated version of the new electron-diffraction tomography technique combined with the precession of the electron beam.

The Sarrabusite structure is monoclinic and consists of (010) layers of straight chains formed by alternating edge-sharing CuO_4Cl_2 and PbO_8 polyhedra parallel to the c axis, which share corners laterally with two zig zag corner-sharing chains of PbO_6Cl_2 and PbO_4Cl_4 bicapped trigonal prisms.

figure 2

PROJECTIONS OF THE SARRABUSITE STRUCTURAL MODEL OBTAINED WITH MANUALLY COLLECTED DATA

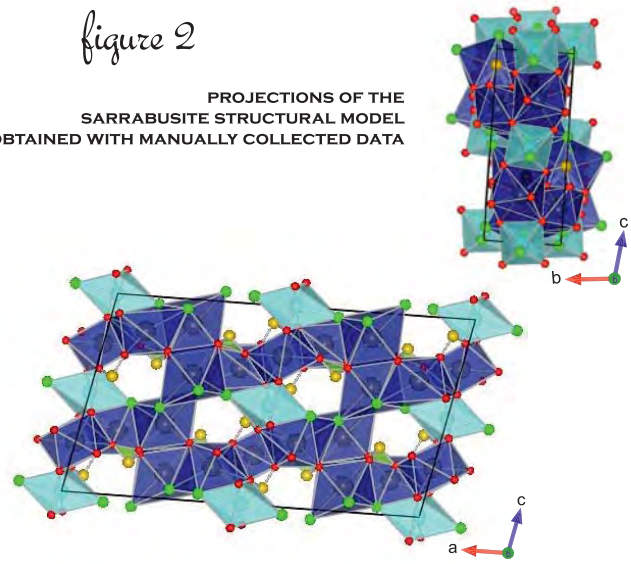

M. Gemmi et al *Acta Cryst.* (2012) B68, 15–23

Bio-mineralization Process in Sea Environment

Intracellular nanorods have been considered as precursors of mature spicules

sponge

Among the siliceous sponges, the spiculogenesis in the demosponge (*Suberites domuncula*) is best understood. It was suspected that the initial stages of spicule formation proceed intracellularly. Because the synthesis of the spicules is a rapid process, the earliest stages of spicule formation can be studied under in vitro conditions in the cell culture system, the primmorphs.

Investigation of nanorods that appear inside the axial filament in the first stages of spicule formation, has been recently performed. Such nanofeatures are not accessible by X-ray techniques and can be investigated only by electron microscopy. One major advantage of electron microscopy is the potential to collect imaging and diffraction data sequentially from the same sample.

The challenge:	small amount of material inside embedded organic tissues
Solution:	Automated 3D diffraction Tomography, EDX and HRTEM

The nanorods with 20 nm diameter and 200 nm length are present intracellularly in the early and initial stages of axial filament formation. The nanorods are then surrounded by a multifunctional polymeric matrix that is the axial filament and silicatein molecules. These nanorods show a typical size of 300–600 nm in length and 20–50 nm in width and were studied by HRTEM, EDX and 3D electron diffraction tomography / PED methods.

By EDX analysis the following stoichiometry was obtained: $Si_{3.86}Al_{2.00}Mg_{0.34}K_{0.16}$ $Fe_{0.16}O_{11}$. 3D diffraction tomography data collection led to the determination of the cell vectors and the space group, C2/c, of the structure. Moreover the electron diffraction and images indicated a two layer phyllosilicate structure. Phyllosilicates are layer silicate made of alternating sheets of Si_2O_5 tetrahedra and $(Al,Mg,Fe)_2(OH)_2$ octahedra. The d-spacing of 20 Å of parameter c indicates a TOT–TOT stacking sequence. In particular, lattice parameters and composition fit the mineral smectite. These types of minerals have been widely identified in marine environments and were occasionally linked to biological activity. The crystalline structure was localized within the organic axial filament of the primordial spicules. It is proposed that this crystalline structure acts as an inorganic template and gives shape and orientation to the newly forming spicule. Thanks to the applied techniques the crystalline nanorods could be detected and analysed, thus moving one step closer to the starting point of spicule biosilicification. These results contribute to the understanding of biosilicification in sponges and might help to provide new insight for bio-nanotechnological applications with potential in the biomimetic and biomedical field.

Crystal Structure

$Si_{3.86}Al_{2.00}Mg_{0.34}K_{0.16}$ $Fe_{0.16}O_{11}$

Monoclinic C2/c
a= 5.18 Å
b= 9.13 Å
c= 20.20 Å
β= 96°

Experimental data

tilt range: ±30°step: 1°

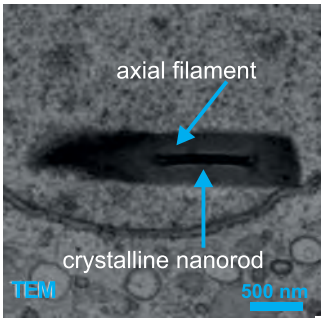

INITIAL FORMATION OF AN AXIAL FILAMENT THAT COMPRISES A CRYSTALLINE NANOROD

figure 1

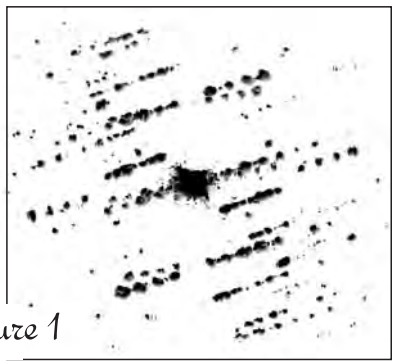

3D RECONSTRUCTION MAP FROM THE SELECTED NANOROD

figure 2

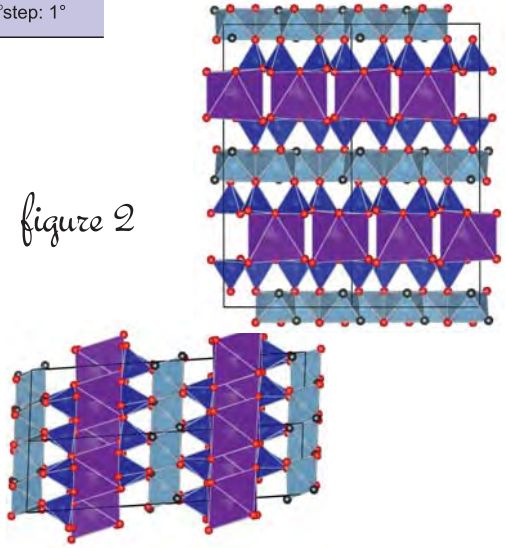

CRYSTAL STRUCTURE OF $Si_{3.86}Al_{2.00}Mg_{0.34}K_{0.16}$ $Fe_{0.16}O_{11}$

E. Mugnaioli et al *ChemBioChem* (2009) 10 683 – 689

What is Stacking in Our Pipes : The Structure of Vaterite

Vaterite is metastable phase of calcium carbonate at ambient conditions at the surface of the earth & is responsible for stacking problems in the pipes

scales in pipes

Vaterite, one of the common natural CaCO3 polymorphs, plays a pivotal role in weathering and biomineralization processes. Vaterite is important for the problems of scales in pipes, biomineralization of mollusks and pearls. Differently from calcite and aragonite (CaCO3 polymorphs), vaterite can be found only in the form of nanosized crystals, not suitable for structure determination by X-Ray diffraction. The structure of vaterite is still an unsolved dilemma (has eluded

The challenge:	Vaterite consists of single crystal aggregates with size of 50 nm or less
Solution:	Automated 3D Diffraction Tomography with precession diffraction

structure determination for almost 100 years!) despite its common occurrence, its relevance in biomineralization processes and the impressive number of published studies around the subject .

All previous structural models for vaterite derived from X-Ray diffraction show geometrically related cells that are difficult to distinguish on the basis of the low-quality data available for nanocrystalline vaterite. Here we report for the first time ab initio determination of vaterite structure from precession electron diffraction data collected via the 3D diffraction tomography approach. Completed 3D diffraction data were available from a single vaterite nanocrystal (50 nm or less).The structure of vaterite was determined in monoclinic space group C2/c and is characterized by a layer arrangement of Ca^{2+} ions alternated by $\{CO_3\}^{2-}$ groups. This structure is consistent with the Raman spectra and a number of experimental findings reported by previous authors.

All analysed vaterite nanocrystals showed stacking disorder and local modulation. The modulation was described by a 6-layer superstructure triclinic cell, resulting in a more satisfactory fit to synchrotron powder diffraction data.The structure was solved ab-initio by direct methods in the triclinic space group C-1.The structure is similar to the two-layer monoclinic model with the same basic motif of Ca^{2+} layers connected to orthogonal $\{CO_3\}^{2-}$ groups.

Local atomic coordination is preserved. Electron diffraction tomography showed its geat potential for studying the structure of nanomaterials that elude conventional methods because of small crystal size, low purity, structural complexity or low availability.

Crystal Structure

$Ca_{1.5}C_{1.5}5O_{4.5}$ (2-layer model)	$Ca_9C_9O_{27}$ (6-layer model)
Monoclinic C2/c	**Triclinic C-1**
a= 12.17 Å	a= 12.17 Å
b= 7.12 Å	b= 7.12 Å
c= 9.47 Å	c= 25.32 Å
β= 118.94°	α= 90°
	β= 99.12°
	γ= 90°

Experimental data

tilt range: ±60° step: 1°
No ind. reflections: 416
No ind. atoms: 45
R = 34%

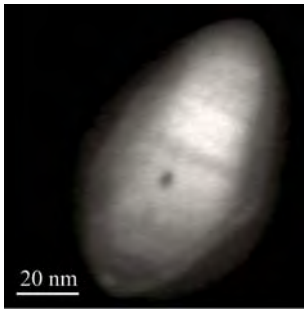

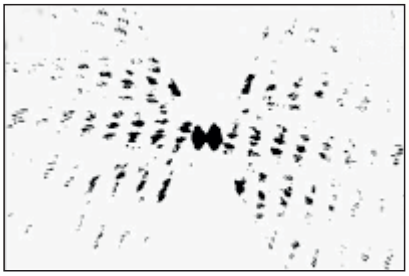

figure 1

STEM IMAGE OF VATERITE NANOPARTICLE (LEFT)
3D RECIPROCAL SPACE RECONSRUCTED FROM ADT DATA
VIEW DOWN THE TILT AXIS (DOWN) MONOCLINIC CELL

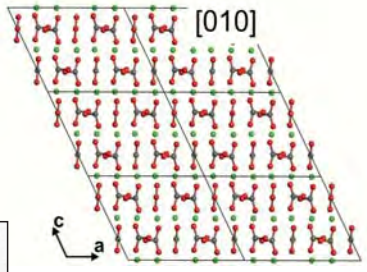

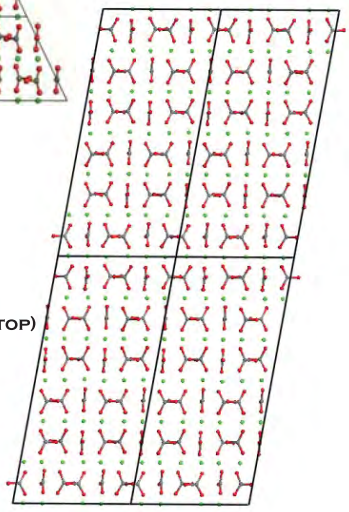

figure 2

CRYSTAL STRUCTURE OF VATERITE 2-LAYER MODEL (TOP) & 6-LAYER MODEL (DOWN)

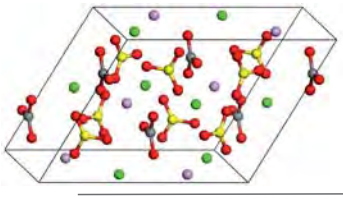

E. Mugnaioli et al *Angew. Chemie Int Ed* (2012) 51 7041-7045

Structure of Embedded Nanodomains in Intermetallics

Ni-Te system is possible applied in thermoelectric generators converting heat into electrical power

Ni-Te is an intermetallic compound with possible applications in thermoelectric generators (TEGs) that convert heat into electrical power by exploiting a temperature gradient. $Ni_{1+x}Te_1$ system is a two-solid phase mixture where nanodomains of modulated (layered) unknown phase (phase b) were found inside the NiTe matrix. Despite many attempts to solve this unknown Ni-Te phase b, its structure and stoichiometry was revealed only using 3D diffraction tomography coupled to precession electron diffraction (PED).

The challenge:	Embedded nanodomains with size up to 70nm, two Ni-Te phases
Solution:	Automated 3D Diffraction Tomography combined to Precession electron diffraction

3D diffraction tomography data were collected on the edge of a milled particle, revealed the presence of two phases, the matrix Ni_1Te_1 (phase α) and the superstructure Ni5Te4 (phase β). Structure determination of the modulated β phase was hampered by the small dimensions of the domains and the fact that most of them are embedded into the Ni_1Te_1 matrix. Reflections coming from the superstructure were recognized and showed a doubling of both c and a parameters, leading to an monoclinic. It is found out that is locally similar to NiTe, but there is a shift of one Te layer by (1/3, 1/3, 0) every two c-periods referred to the initial hexagonal NiTe-type structure.

The analysis of the experimental data confirms that Ni_1Te_1 (phase α) has a hexagonal structure, of NiAs type, where the Te atoms form a BCBC... hexagonal sequence. The remaining Ni atoms are distributed over octahedral sites between the Te Layers (figure 2).

The new Ni_5Te_4 (phase β) has a monoclinic structure where the Te atoms form a sublattice with BABCBA... hexagonal sequence, while the Ni atoms occupy deformed octahedral sites with a $...c_oc_oa_oa_oc_o...$ sequence and tetrahedral sites with a $...c_tb_tc_t...$ sequence. It is found out that is locally similar to NiTe, but there is a shift of one Te layer by (1/3, 1/3, 0) every two c-periods referred to the initial hexagonal NiTe-type structure.

ADT together with PED allowed the structure determination of the nickel-rich phase superstructure Ni_5Te_4 (phase β) for the first time.

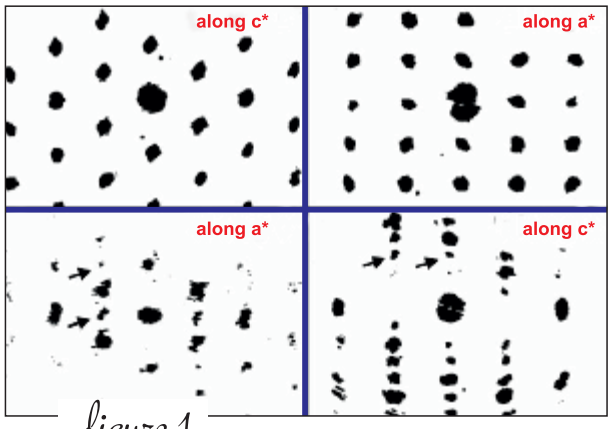

figure 1

Projections of the reconstructed 3D diffraction of phase α along the c* & the a* axis; (top, hexagonal) phase β along the c* & the a* axis (down, Moniclinic) Superstructure reflections are marked with Black arrows.

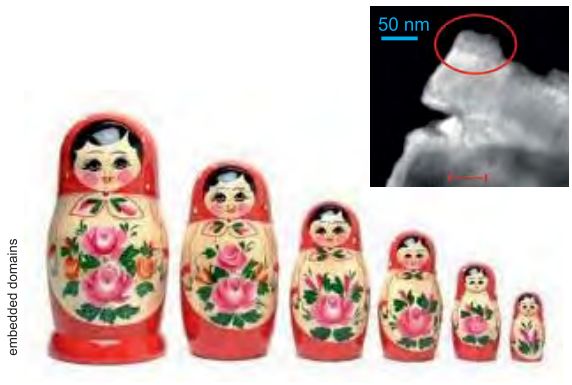

Crystal Structure

	Ni_1Te_1 (α-phase)	Ni_5Te_4 (β-phase)
	Hexagonal $P6_3/mmc$	**Monoclinic Pm**
a=	3.85 Å	6.95 Å
b=	3.85Å	4.02 Å
c=	5.22 Å	11.96 Å
α=	90°	90°
β=	90°	90°
γ=	120°	90°

Experimantal data

Ni_1Te_1 / Ni_5Te_4
tilt range: ±50° / ±40° step: 1°
No ind. reflections 47 / 411
No ind. atoms 2 / 11
R = 22.3% / 24.6%

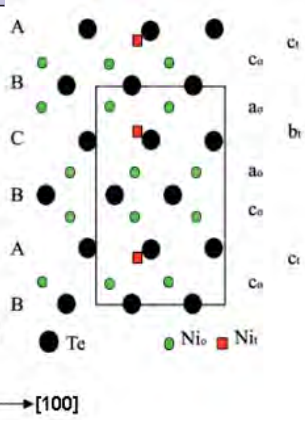

figure 2

Crystal structure Ni_1Te_1 (phase α) and Ni_5Te_4 (phase β , down)

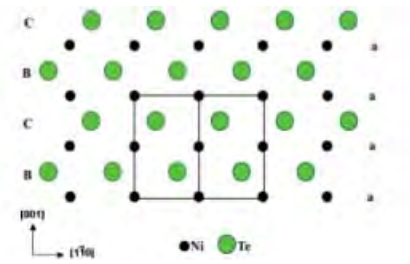

E. Sarakinou et al *Semiconductor Science and Technology* (2012) 27 105003

RESEARCH GROUPS & TECHNICAL DETAILS

STRUCTURE OF INTRIGUING MESO-MICROPOROUS ZEOLITES

Technical details:
single tilt cryo-holder; beam precession (1.2°) by DigitStar, NanoMEGAS.
Research Group:
Institut für Physikalische Chemie der Johannes Gutenberg-Universität, Mainz, Germany;
Instituto de Tecnología Química, Universidad Politécnica de Valencia, Spain.

FROM "CLEAN ENERGY" CARS TO STRUCTURE OF METAL-ORGANIC FRAMEWORK MATERIALS (MOFS)

Technical details:
single tilt cryo-holder; beam precession (1.2°) by DigitStar, NanoMEGAS.
Research Group:
Institut für Physikalische Chemie der Johannes Gutenberg-Universität, Mainz, Germany.

TOWARDS ALTERNATIVE ENERGY SOURCES: STRUCTURE OF THERMOELECTRIC NANOMATERIALS

Technical details:
rotational tomographic holder; beam precession (1.2°) by DigitStar, NanoMEGAS.
Research Group:
Institut für Physikalische Chemie der Johannes Gutenberg-Universität, Mainz,

STRUCTURE OF PIGMENT YELLOW FOR CAR INDUSTRY

Technical details:
double-tilt rotational holder; XRPD and real space methods.
Research Group:
Institut für Anorganische und Analytische Chemie, Goethe Universität, Frankfurt am Main, Germany; Institut für Physikalische Chemie der Johannes Gutenberg-Universität, Mainz, Germany.

SHED LIGHT TO MAGMA GENESIS & SEISMICITY

Technical details:
rotational tomographic holder; beam precession (1.2°) by DigitStar, NanoMEGAS.
Research Group:
Istituto di Scienze della Terra, Università degli Studi di Milano, Italia;
Institut für Physikalische Chemie der Johannes Gutenberg-Universität, Mainz, Germany.

STRUCTURE OF NEW SARRABUSITE MINERAL

Technical details:
single-tilt holder; beam precession (1.0°) by SpinningStar, NanoMEGAS.
Research Group:
Istituto di Scienze della Terra, Università degli Studi di Milano, Italia;
Institut für Physikalische Chemie der Johannes Gutenberg-Universität, Mainz, Germany.

WHAT IS STACKING IN OUR PIPES : THE STRUCTURE OF VATERITE

Technical details:
rotational tomographic holder; beam precession (1.2°) by DigitStar, NanoMEGAS.
Research Group:
Institut für Physikalische Chemie der Johannes Gutenberg-Universität, Mainz,

ARCHITECTURE OF HYBRID NANOCRYSTALLINE MICROPOROUS MATERIALS

Technical details:
rotational tomographic holder; beam precession (1.2°) by DigitStar, NanoMEGAS.
Research Group:
ENI s.p.a. — Refining & Marketing Division, Milano, Italy;
Institut für Physikalische Chemie der Johannes Gutenberg-Universität, Mainz, Germany.

INSIDE THE STRUCTURE OF DYE-SENSITIZED SOLAR CELLS

Technical details:
rotational tomographic holder; beam precession (1.2°) by DigitStar, NanoMEGAS.
Research Group:
Institut für Physikalische Chemie und Institut für Anorganische Chemie und Analytische Chemie der Johannes Gutenberg-Universität, Mainz, Germany.

INSIDE THE STRUCTURE OF PHOSPHOR-CONVERTED LIGHT-EMITTING DIODES (LED)

Technical details:
rotational tomographic holder; beam precession (1.2°) by DigitStar, NanoMEGAS.
Research Group:
Institut für Physikalische Chemie der Johannes Gutenberg-Universität, Mainz, Germany;
Institut für Chemie, Ludwig-Maximilians-Universität, Munich, Germany.

STRUCTURE OF ORGANIC (CNBA) MOLECULES

Technical details:
rotational tomographic holder; beam precession (1.2°) by DigitStar, NanoMEGAS.
Research Group:
Institut für Physikalische Chemie der Johannes Gutenberg-Universität, Mainz,

CHAROITE: THE ENIGMATIC STRUCTURE OF "UNNATURALLY BEAUTIFUL" GEMSTONE

Technical details:
rotational tomographic holder; precession (1.3°) by SpinningStar, NanoMEGAS.
Research Group:
Institut für Physikalische Chemie der Johannes Gutenberg-Universität, Mainz, Germany;
Department of Crystallography, Saint Petersburg State University, Russia.

BIO-MINERALIZATION PROCESS IN SEA ENVIRONMENT

Technical details:
double-tilt holder
Research Group:
Institut für Physikalische Chemie und Institut für physiologische Chemie der Johannes Gutenberg-Universität, Mainz, Germany.

STRUCTURE OF EMBEDDED NANODOMAINS IN INTERMETALLICS

Technical details:
rotational tomographic holder; beam precession (1.2°) by DigitStar, NanoMEGAS.
Research Group:
Institut für Physikalische Chemie der Johannes Gutenberg-Universität, Mainz,

Automatic 3D diffraction tomography has been performed in a FEI TECNAI F30 S-Twin

We would like to acknowledge Prof. U. Kolb , Dr. E. Mugnaoli (Univ Mainz)
and Dr. M. Gemmi (IIT Pisa) for figures selection in the application notes.

NanoMEGAS

Advanced Tools for electron diffraction

NanoMEGAS SPRL

Blvd Edmond Machtens 79

B-1080 Brussels

Belgium

www.nanomegas.com

info@nanomegas.com